

Elasticity and thermal expansivity of $(\text{AgI})_x(\text{AgPO}_3)_{1-x}$ glasses

R. Bogue and R. J. Sladek

Department of Physics, Purdue University, West Lafayette, Indiana 47907

(Received 8 January 1990; revised manuscript received 2 April 1990)

We have measured the transit times of longitudinal and shear ultrasonic waves in $(\text{AgI})_x(\text{AgPO}_3)_{1-x}$ glasses, with $0 \leq x \leq 0.46$, at temperatures between 80 and 360 K and at pressures up to 4 kbar at 196 K and/or 296 K. We have also measured the thermal expansivity of $(\text{AgI})_x(\text{AgPO}_3)_{1-x}$ glasses with $x = 0$ and 0.31 between 90 and 295 K. From the transit-time data, we found that all the elastic stiffness moduli decrease with increases in AgI content or temperature. However, all moduli increase with increasing pressure. The shear-to-bulk modulus ratio, C_T/B , is close to 0.25, the value calculated by Bergman and Kantor for a material having a one-dimensional backbone and an interstitial fluid near the percolation limit. The C_T/B ratio decreases as AgI content or pressure increases, indicating a reduction in structural stability and that a structural phase transition involving macroscopic shear may occur at high pressure. The temperature dependence of each elastic modulus has a component due to elastic anharmonicity and, in some samples, an inflection due to Ag-ion relaxation which occurs at a lower temperature the higher the AgI content. The pressure dependences of the elastic moduli yielded positive ultrasonic mode Grüneisen parameters and an average high-temperature Grüneisen parameter greater than the mode Grüneisen parameters deduced from the temperature dependences of the moduli or from thermal expansion data. While the latter Grüneisen parameters agreed at room temperature the thermal Grüneisen parameters fell as temperature decreased and became negative at about 155 K for the $x = 0$ sample, indicating the importance of excitations having a negative anharmonicity parameter (mode Grüneisen parameter).

I. INTRODUCTION

Fast-ion conducting glasses have drawn substantial interest in recent years,¹ both because of their possible use as solid electrolytes and because they offer the theoretical challenge of understanding how a disordered structure could affect the fast-ionic dynamics. Several studies have focused on phosphate or borate glass systems combined with a metal halide, usually AgI or LiI, due to their high ionic conductivities, stability, and relative resistance to attack by moisture. These materials can be readily obtained as glasses merely by quenching their melts to room temperature.

The system of $(\text{AgI})_x(\text{AgPO}_3)_{1-x}$ glasses has been of particular interest. These glasses can be produced in a wide range of compositions ($0 \leq x \leq 0.60$) without need for fast-quenching techniques.² Rapid quenching extends this range up to 80 mol % AgI.³ Their ionic conductivity at room temperature is relatively high (e.g., $0.11 \Omega^{-1} \text{m}^{-1}$ for $x = 0.4$),⁴ and can be further enhanced³ by mixing with B_2O_3 . Such mixed glasses have found commercial application as electrolytes in low-current, long-shelf-life batteries.

Elastic measurements on $(\text{AgI})_x(\text{AgPO}_3)_{1-x}$ glasses have hitherto involved low-frequency (≤ 110 Hz) mechanical-vibration measurements² or Brillouin scattering of light.⁵ The former yielded values for Young's modulus (at low frequencies) while the latter yielded results at hypersonic frequencies (5–12 GHz). The velocity values deduced from the latter suffered from uncertainty in how well the dielectric constant was known.

To obtain more complete and accurate information about the elastic constants of $(\text{AgI})_x(\text{AgPO}_3)_{1-x}$ glasses,

we measured, and report herein, the results of measurements of the transit times of both longitudinal and shear ultrasonic waves at various temperatures and pressures. From these results (and our thermal-expansivity data, when necessary) we deduce the elastic stiffness moduli of each type of wave and use them to calculate the bulk modulus.

The behavior of the ultrasonic velocity as a function of temperature may involve two difficult-to-separate contributions: (1) anharmonic effects and (2) thermally activated relaxation processes of the fast Ag^+ ions, which were discussed in detail elsewhere.⁶ Therefore we have determined the derivatives of the elastic moduli as functions of hydrostatic pressure at 196 K and/or 296 K.

II. EXPERIMENTAL DETAILS AND DATA ANALYSIS

A. Sample preparation

The $(\text{AgI})_x(\text{AgPO}_3)_{1-x}$ samples used in this study were prepared by C. Liu of the Department of Chemistry of Purdue University by methods described elsewhere.² The samples produced were 5–6-mm-thick clear disks, with a yellow tint that became more pronounced with increasing AgI concentration.

Each sample was polished against a flat plate using a succession of silicon carbide and alumina powders in water suspension. In this way, opposite faces were prepared flat to within two interface fringes of helium light, and parallel to within 10^{-4} rad.

Densities were measured at room temperature by immersion in distilled water and are shown in Table I. Sample lengths were determined using a micrometer and also

TABLE I. Room-temperature characteristics of $(\text{AgI})_x(\text{AgPO}_3)_{1-x}$ glass samples used in this study.

Sample x	Density (g/cm^3)	C_L ($10^{11} \text{ dyn}/\text{cm}^2$)	C_T	$\frac{\partial C_L}{\partial P}$	$\frac{\partial C_T}{\partial P}$
0.00	4.449	4.99	0.992	8.47	0.73
0.11	4.675	4.67	0.902	9.60	0.89
0.21	4.852	4.29	0.826	9.68	0.88
0.31	5.048	3.99	0.751	9.37	0.85
0.39	5.263	3.72	0.677	9.73	0.78
0.41	5.256	3.49	0.635	10.02	0.79
0.46	5.320	3.45	0.591	10.49	0.70

using an electronic gauge and standard gauge blocks. Lengths could be determined to within ± 0.0003 cm.

Each sample was inspected visually under a binocular microscope. The focal plane of the microscope was moved up and down to allow defects to be viewed throughout the material. All samples had a few bubbles in them of diameter $\leq 50 \mu\text{m}$, presumably stemming from the act of pouring the molten glasses into the brass mold. We estimate that there were about 100 bubbles per cubic centimeter, so that scattering from them would be expected to produce a contribution to the ultrasonic attenuation⁷ of less than 0.05 cm^{-1} and not enough phase shift to significantly affect the echo-overlap frequency significantly. This attenuation contribution is small compared to the total measured attenuation.⁶

The fractional concentration of AgI in each sample was determined by means of x-ray fluorescence using the Kevex XRF-0700 and the Kevex Micro-X700 analytical spectrometer of the Purdue University National Science Foundation Materials Research Laboratory (NSF-MRL) Central Analysis Facility. This yielded a value of x accurate to within ± 0.01 . Our x values were very close to those expected from preparation information provided by Liu,⁸ who suggested, however, that a small loss of P_2O_5 gas might have occurred during preparation in some cases. From our concentration determinations any such loss must have been insignificant.

B. Thermal expansion

A commercial quartz-pushrod dilatometer (Dilatronic Model 201C) was used to measure the change of sample length as temperature was lowered below 296 K by suspending the assembly in the gas chamber of a Dewar containing liquid nitrogen. Temperature was monitored with a copper-Constantan thermocouple, which was attached to the sample with masking tape.

The dilatometer was calibrated by measuring the contraction of a copper standard (NBS standard reference material 736) and comparing the result to published NBS values. The differences between the values we measured for copper and the NBS values were used to correct the values we measured for our glass samples. The corrected glass values differed by less than 10% from the measured values. We estimate a $\pm 5\%$ accuracy for the corrected glass expansivity values.

C. Ultrasonic experiments

Commercial X-cut and ac-cut quartz transducers (Valpey Crystal Corporation) plated with chrome gold were used to convert the rf input pulses to longitudinal and shear ultrasonic pulses, respectively. Dow Corning 276-V9 resin and 200 fluid served as the bonding agents.

The sample, with attached transducer, was mounted in a spring-loaded sample holder and suspended in a nitrogen Dewar. By evacuating the Dewar, the cooling rate could be held to less than $0.5^\circ\text{C}/\text{min}$, allowing data to be obtained while cooling. Temperature was monitored by measuring the voltage drop across a calibrated platinum resistor carrying a constant $100 \mu\text{A}$ current.

Longitudinal and shear wave velocities (V_L and V_T , respectively) were determined from the transit times of ultrasonic waves using the pulse-echo-overlap technique.^{9,10} With some care, changes in the velocity could be determined to within a few parts in 10^5 . However, the absolute values of the transit time and the velocity of the ultrasonic wave pulse were much less accurate due to vagaries in the thickness of the material bonding the transducer to the sample. When a transducer was removed and reattached, the observed overlap frequency sometimes shifted by as much as 0.1%.

Our velocity results were used with our density data and thermal-expansivity results to calculate the longitudinal, shear, and bulk elastic moduli (C_L , C_T , and B , respectively) using the formulas

$$C_L = \rho V_L^2, \quad (1)$$

$$C_T = \rho V_T^2, \quad (2)$$

$$B = C_L - \frac{4}{3}C_T, \quad (3)$$

where ρ is the density.

Hydrostatic pressure was applied to our $x=0$ and 0.31 samples by means of motor oil at 296 K, or an isopentane-pentane mixture at 196 K. The pressure fluid was supplied to the cylindrical steel pressure vessels in which the sample was mounted by means of a commercial (Aminco) pump and pressure intensifier system. Pressures were measured by means of a Bourdon Gauge. Cook's method¹¹ was employed to correct the transit-time data for changes in the sample's size due to pressure.

Since the pressure dependences of the elastic moduli of crystalline, wurtzite phase AgI exhibit considerable hysteresis in this pressure regime,¹² overlap frequencies were

measured at closely spaced intervals while both increasing and decreasing pressure. No hysteresis was observed in any of our samples.

III. RESULTS AND DISCUSSION

A. Thermal expansivity

We measured the length change of two of our samples from 295 K down to 90 K. The results of our AgPO_3 glass sample are shown in Fig. 1. Data on our $(\text{AgI})_{0.31}(\text{AgPO}_3)_{0.69}$ glass sample were generally similar but exhibited more scatter and are not shown to avoid clutter. We found that the thermal-expansion coefficient, defined as

$$a(T) = \frac{1}{l_{295\text{K}}} \frac{dl}{dT}, \quad (4)$$

is $(23 \pm 1) \times 10^{-6} \text{ K}^{-1}$ for both AgPO_3 glass and $(\text{AgI})_{0.31}(\text{AgPO}_3)_{0.69}$ glass at room temperature. This value remains fairly constant down to 200 K, where it begins to fall, and passes through zero at about 153 K for AgPO_3 and at about 140 K for the 31 mol % AgI sample. At 100 K the coefficient for both samples is $-20 \times 10^{-6} \text{ K}^{-1}$. No previous thermal expansivity measurements have been reported for $(\text{AgI})_x(\text{AgPO}_3)_{1-x}$ glasses or even for crystalline AgPO_3 .

The thermal expansions of the two samples were so similar, in spite of their different concentrations, that it was deemed unnecessary to measure additional samples. These results indicate that the thermal expansion is dominated by the presence of chains of corner-connected PO_4 tetrahedra in $(\text{AgI})_x(\text{AgPO}_3)_{1-x}$ glasses,^{13,14} and is not greatly affected by the presence of as much as 31 mol % AgI.

Thermal-expansion data can be used to calculate a thermal Grüneisen parameter from experimental quantities (if their values are known) by means of the relation

$$\gamma_{\text{th}} = 3aVB_T/C_v = 3aVB/C_p, \quad (5)$$

where a is the linear-expansion coefficient, V is the volume, B_T is the isothermal bulk modulus, B the adia-

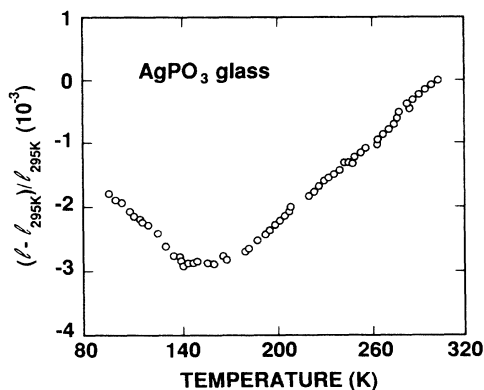


FIG. 1. The thermal expansivity of AgPO_3 glass as a function of temperature.

batic bulk modulus, and $C_{v,p}$ are the heat capacities at constant volume and pressure, respectively.

Since heat-capacity data are lacking for our samples, we deduced values for γ_{th} at various temperatures by using the Debye heat capacity calculated from the elastic Debye temperature Θ_{el} obtained from our ultrasonic velocity data (see Sec. III C). This yielded $\gamma_{\text{th}}(295 \text{ K})$ of 0.85 for AgPO_3 glass and 0.66 for $(\text{AgI})_{0.31}(\text{AgPO}_3)_{0.69}$ glass. The value for AgPO_3 glass agrees well with the 0.90 value deduced from our elastic constant versus temperature data using a quasiharmonic model as we shall see later. We have also deduced γ_{th} at other temperatures for AgPO_3 glass. We found that γ_{th} increased monotonically with temperature, being -0.90 at 100 K, 0 at 153 K, and 0.86 at 200 K. For comparison we note that the -0.90 value of γ_{th} occurs at $T/\Theta \approx 0.04$ for vitreous SiO_2 .

A "microscopic" interpretation of γ_{th} is usually made in terms of various contributions, each of which depends on the product of an anharmonicity parameter γ_i and heat capacity C_{v_i} of the entities involved, i.e.,

$$\gamma_{\text{th}} = \frac{\sum_i \gamma_i C_{v_i}}{\sum_i C_{v_i}}. \quad (6)$$

Equation (6) allows us to understand why γ_{th} can be negative at the lower temperatures even though our ultrasonic velocity versus pressure data indicate that long-wavelength acoustic modes have positive Grüneisen parameters (see Sec. III E). Namely, there are entities with a quite negative Grüneisen parameter (perhaps ≈ -10) which are relatively more important at the lower temperatures than are optical modes or long-wavelength acoustic modes. Although the nature of the negative Grüneisen parameter entities is unknown, they might be transverse-acoustic vibrations in the dispersive, short wavelength part of the phonon spectrum. These vibrations could be represented by Einstein oscillators whose characteristic temperature Θ_{TA}^E is much less than that deducible from the velocity of the transverse ultrasonic waves reported herein. Unfortunately, we do not have enough information about the phonon spectra of our glasses to be able to utilize Eq. (6) in a more quantitative fashion. It should be noted that the above suggestion for the nature of the negative Grüneisen parameter entities is similar to that used for Ge and Si crystals¹⁵ although their corresponding modes have much less negative Grüneisen parameters. We wonder, if the glassy nature of our samples is responsible for their quite negative Grüneisen parameters. One consequence of the glass structure of our AgPO_3 sample is that its density is about 4% less than that reported¹⁶ for crystalline AgPO_3 . This density defect is larger than that estimated from the bubble concentration referred to in Sec. II A.

Very negative Grüneisen parameter values have been associated with the presence of two-level systems (TLS) (ionic hopping in double-potential wells) in SiO_2 glass. Thus the reader might ask, "Could not your negative Grüneisen parameter entities arise from such systems?"

Our answer is that we do not think so, since in SiO_2 and other glasses the TLS have a range of small energy separations whose density is constant from zero to some small maximum value. This results in a heat-capacity contribution which is proportional to temperature. The γC_D product for such TLS would have to be so negative to explain our thermal expansivity at lower temperatures that it could not be overcome by the contributions from entities with positive Grüneisen parameters at the higher temperatures which are necessary to account for the observed positive thermal-expansion region. On the other hand, the contribution from a monoenergetic TLS, with a suitably negative Grüneisen parameter, could be made to account for our data provided that it had an unphysically large energy-level separation.

Before closing this section we warn the reader not to attribute too much significance to the different temperature at which the length of each sample reaches a minimum (and the expansion coefficient α crosses zero), because of the great uncertainty in the data in that temperature range. Nevertheless, the presence of AgI appears to push the transition to negative expansion down to slightly lower temperature, perhaps due to long-wavelength modes having larger positive Grüneisen parameters and smaller Debye temperatures (and hence larger heat capacities at a given temperature) in the AgI doped sample (see Table III).

B. Velocities and elastic moduli

Ultrasonic velocities were obtained from transit times of 5-MHz ultrasonic waves and used to determine the elastic stiffness moduli of $(\text{AgI})_x(\text{AgPO}_3)_{1-x}$ glasses with various AgI concentrations at room temperature. A few samples were also measured at 2, 10, and 15 MHz. We observed no frequency dependence in the velocities or elastic moduli other than that due to the Ag^+ relaxation described below.

The elastic moduli decreased nearly linearly with increasing AgI content (see Table I and Fig. 2) even though the density increases with AgI content. The observed values for the longitudinal and shear elastic moduli at $x \leq 0.3$ compare favorably with those determined from Brillouin scattering by Börjesson *et al.*,⁵ although the accuracy of their values is limited by the necessity to know the refractive index to deduce them.

At the higher concentrations our elastic moduli are lower than those of Börjesson *et al.* (they found $C_L = 3.87$ and 3.56×10^{10} dyn/cm², $C_T = 7.0 \times 10^{10}$ and 6.6×10^{10} dyn/cm² for $x = 0.4$ and 0.5 , respectively). This reflects the fact that, at room temperature, ultrasonic waves in our samples with similar concentrations are damped by the motion of the mobile Ag ions, whereas Brillouin scattering operates in the unrelaxed, high-frequency range. After we corrected for this, our and their values for samples with $x = 0.4$ agree to within their combined experimental uncertainties (4%).

Also, for comparison, we may consider 5-MHz velocities determined by Carini *et al.* for $(\text{AgI})_x(\text{Ag}_2\text{O} \cdot 4\text{B}_2\text{O}_3)_{1-x}$ glasses.¹⁷ These borate glasses are also fast-ionic conductors, with conductivities compa-

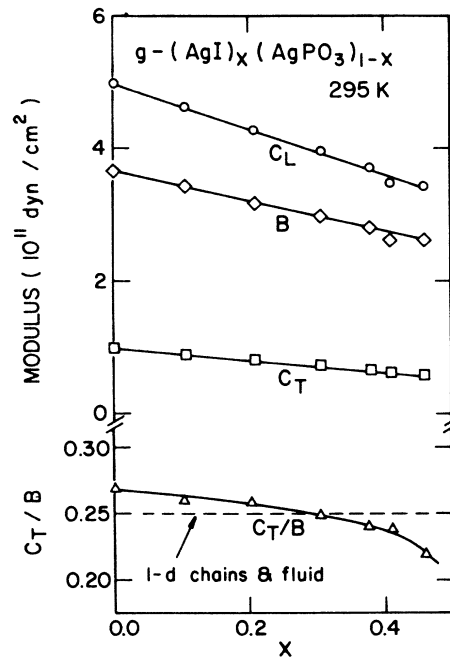


FIG. 2. The longitudinal, transverse, and bulk elastic moduli and the shear-to-bulk modulus ratio in $(\text{AgI})_x(\text{AgPO}_3)_{1-x}$ glasses at room temperature for several values of x . The moduli were deduced from the transit times of 5-MHz ultrasonic waves.

table to those of the phosphate glasses, although they do not contain long chains of oxide groups. The longitudinal wave velocity for the $x = 0$ borate glass is 4.25×10^5 cm/s, and the shear wave velocity is 2.26×10^5 cm/s. As AgI is added, the longitudinal and shear velocities fall to 3.42×10^5 and 1.81×10^5 cm/s, respectively, for $x = 0.55$.

The transit times of longitudinal and shear waves of our $(\text{AgI})_x(\text{AgPO}_3)_{1-x}$ glasses were also measured as a function of temperature at 2 and 5 MHz for our $x = 0, 0.11, 0.31,$ and 0.39 samples. Our results were used with the thermal expansivity and density data to calculate the longitudinal and shear elastic stiffness moduli as functions of temperature using Eqs. (1) and (2) (see Figs. 3 and 4).

From Fig. 2 we see that the ratio C_T/B is 0.27 for the pure AgPO_3 sample. This ratio decreases as x increases, eventually reaching 0.22 at $x = 0.46$. Values of C_T/B range from ~ 0.83 for tetrahedrally coordinated network glasses such as SiO_2 and GeO_2 , through 0.5 for quasi-two-dimensional glasses ($\text{As}_2\text{S}_3, \text{As}_2\text{Se}_3$),¹⁸ to ~ 0.21 for some polymer glasses.¹⁹

Carini *et al.*, report that the ratio of C_T to B is 0.454 for the borate glasses without AgI, which do not contain long chains. This ratio varies nonmonotonically with increasing AgI concentration, but remains in the range 0.446–0.483. Hence, the proximity of our C_T/B ratios to 0.25, especially for the $x = 0.31$ sample, may be considered a feature of the weak cross linking between phosphate chains. The decrease in C_T/B with increasing AgI content is consistent with the loss (or weakening) of cross links between PO_4 chains.

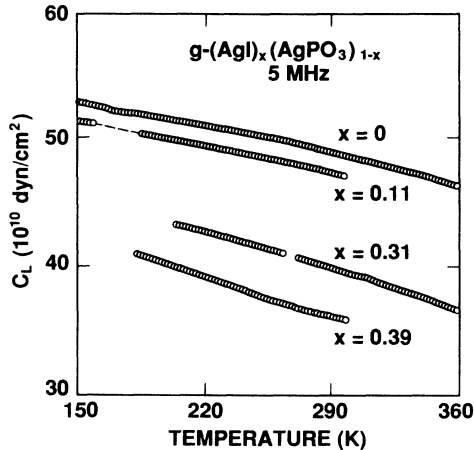


FIG. 3. The longitudinal wave elastic constant C_L of $(\text{AgI})_x(\text{AgPO}_3)_{1-x}$ glasses as a function of temperature. (Deduced from the transit times of 5-MHz ultrasonic waves.)

If we employ an expression due to Bergman and Kantor,²⁰ derived for an inhomogeneous random mixture of fluid and a solid backbone near the percolation limit, our shear-to-bulk modulus ratios can be used to deduce an effective dimensionality d , for each of our glasses

$$d = 4C_T/B. \quad (7)$$

Using the C_T/B values in Fig. 5, we find that d decreases from 1.07 for our AgPO_3 sample to 0.89 for our $(\text{AgI})_{0.46}(\text{AgPO}_3)_{0.54}$ sample, having passed through a value very close to unity (1.01) for our $(\text{AgI})_{0.31}(\text{AgPO}_3)_{0.69}$ sample.

Mangion and Johari have deduced⁴ that there is a conductivity percolation threshold at $x=0.3$ for $(\text{AgI})_x(\text{AgPO}_3)_{1-x}$ glasses, implying that at such a concentration there are AgI regions with long-range connectivity. This is in accord with the glasses having chains of PO_4 tetrahedra and near unity dimensionality. Further-

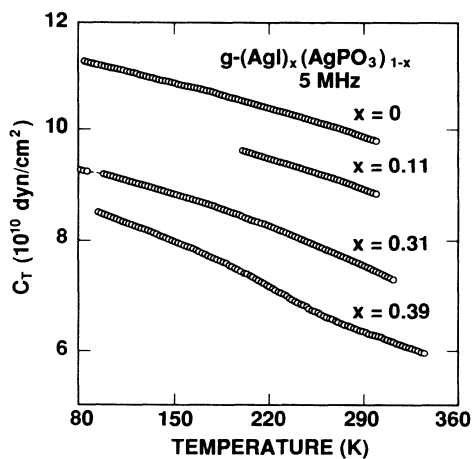


FIG. 4. The shear wave elastic constant C_T of $(\text{AgI})_x(\text{AgPO}_3)_{1-x}$ glasses as a function of temperature. (Deduced from the transit times of 5-MHz ultrasonic waves.)

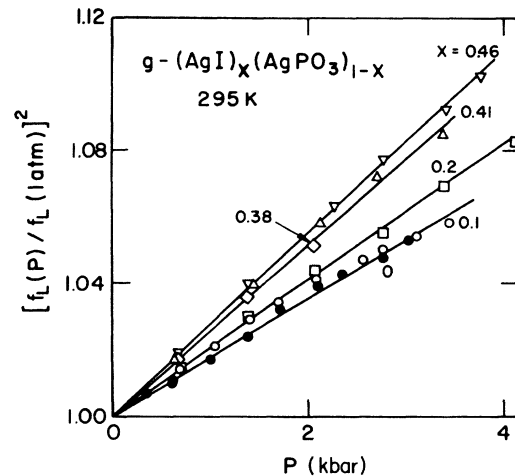


FIG. 5. The pressure dependence of the square of the longitudinal wave echo-overlap frequency, f_L^2 , in $(\text{AgI})_x(\text{AgPO}_3)_{1-x}$ glasses at room temperature for several values of x . All values were measured at 5 MHz.

more, the values of d are consistent with the cross linkage between the PO_4 chains in AgPO_3 being very weak and becoming even weaker when AgI is present. The decrease of d below 1 for $x > 0.3$ may be due to disruption of some of the chains due to iodine ions replacing some of the PO_4 tetrahedra in them.

C. Quasiharmonic softening and Debye temperature

The moduli of all our samples decrease significantly as temperature increases from 100 K to room temperature. Most of the decreases are understandable in terms of a simplified version of the quasiharmonic-atomic-oscillator model developed for crystalline solids in general by Leibfried and Ludwig,²¹ as adapted for cubic crystals by Garber and Granato²² and for isotropic solids by Claytor and Sladek.²³ By assuming that all significant vibrational modes can be represented by an average anharmonicity parameter γ , the longitudinal modulus C_L , and shear modulus C_T , can be expressed as

$$C_L = C_L^0 + \frac{U}{V} \left\{ -\gamma^2 - \gamma \left[\left[\frac{\partial C_L}{\partial P} \right]_T - \frac{C_L}{3B} \right] \right\}, \quad (8)$$

$$C_T = C_T^0 + \frac{1}{V} \left\{ -\gamma^2 (U + C_v T) - \gamma U \left[\left[\frac{\partial C_T}{\partial P} \right]_T - \frac{C_T}{3B} \right] \right\}, \quad (9)$$

where C_L^0 and C_T^0 are the elastic stiffnesses at $T=0$ K, V is the volume, k_B is Boltzmann's constant, and U is the total energy of the atomic oscillations. Using the Debye model for solids, we can estimate values of U and C_v from the relations

$$U = 9Nk_B \Theta (T/\Theta)^4 \int_0^{\Theta/T} \frac{y^3}{e^y - 1} dy, \quad (10)$$

$$C_v = dU/dT, \quad (11)$$

where N is the number of atoms in volume V , Θ is the thermal Debye temperature usually obtained from low-temperature heat-capacity data, and $y = h\nu/k_B T$. Because calorimetric information is not available for $(\text{AgI})_x(\text{AgPO}_3)_{1-x}$ glasses, we used the elastic Debye temperature Θ_{el} obtained from the longitudinal and shear ultrasonic wave velocities V_L and V_T at 296 K by using the relation

$$\Theta_{\text{el}} = \frac{h}{k_B} \left[\frac{3\rho Q N_A}{4\pi W} \right]^{1/3} \left[\frac{1}{3V_L^3} + \frac{2}{3V_T^3} \right]^{-1/3}, \quad (12)$$

where h is the Planck's constant, Q is the number of atoms per formula unit, W is molecular weight, and N_A is Avogadro's number. Using our room-temperature data, we deduced the elastic Debye temperatures presented in Table III. The values range from 208 K for $x=0$ to 135 K for $x=0.46$, and are similar to those of many glasses.

We found that Eqs. (8) and (9) could account for the temperature dependences of the elastic moduli of our AgPO_3 glass sample reasonably well if γ was allowed to increase somewhat with temperature (i.e., from about 0.75 at 80 K to about 0.95 at 295 K). Such a temperature dependence of γ is roughly consistent with the fact that the thermal-expansion coefficient is negative in our $(\text{AgI})_x(\text{AgPO}_3)_{1-x}$ glasses at the lower temperatures and the fact that in As_2S_3 and As_2Se_3 glasses, which do not have such a region, γ decreases as temperature increases.

For our AgPO_3 glass sample the values of γ at 200 and 295 K are within 10% of the values of γ_{th} deduced from our thermal expansivity data in Sec. III A. This is very good agreement considering the necessity of using calculated internal energy and/or heat capacities to obtain Grüneisen parameter values.

On the other hand, for our AgPO_3 glass, γ remains positive and decreases very little with decreasing temperature below 200 K (reaching about 0.75 near 80 K), while γ_{th} exhibits a large decrease and a change of sign in that temperature range, reaching -0.090 at 100 K, as mentioned previously.

The large discrepancy between γ and γ_{th} may be due to the former having been obtained from elastic constant data whose temperature dependence comes mainly from that of the internal energy, i.e., $\int C_v dT$, whereas $\gamma_{\text{th}} \sim 1/C_v$.

D. Ag^+ -ion relaxation

As temperature increases from 100 to 360 K, the value of C_T for the 39 mol% AgI sample decreases from 8.48×10^{10} to 6.00×10^{10} dyn/cm² (see Fig. 4). This decrease is a combination of the normal quasiharmonic softening described above and an additional contribution due to Ag^+ -ion relaxation. This relaxation causes an additional 2.5% decrease in the shear wave velocity over a broad temperature range centered at 240 K.

If the relaxation followed the simple Debye behavior, as discussed in Ref. 6, the decrease in modulus could be described by

$$\frac{C(\omega) - C(\infty)}{C} = \frac{4\alpha_{\text{peak}} V}{\omega} \frac{1}{1 + \omega^2 \tau^2}, \quad (13)$$

where α_{peak} is the additional ultrasonic attenuation at the center of the relaxation, after subtracting background, and V is the ultrasonic velocity. The central temperature at which the relaxation occurs is determined by the inflection in the plot of C_T versus temperature. C_T softens at a higher temperature the higher the measuring frequency.⁶ Equation (13) is not expected to provide a quantitative connection between the modulus depression and the amplitude of the relaxation attenuation (which accompanies the inflection in the modulus). Nevertheless use of it along with the attenuation observed for the $x=0.39$ sample yielded a 4.8% modulus decrease which is surprisingly close to the 5% decrease implied by the 2.5% decrease in velocity.

A velocity decrease due to the Ag -ion relaxation occurs in the $x=0.3$ sample, also. It is also very broad, centered near 295 K, and is not completed at our highest temperature.

E. Effect of pressure on the elastic moduli and structural stability

From Figs. 5 and 6 we see that the square of the echo-overlap frequencies increases linearly with hydrostatic pressure for all concentrations studied. This results in C_L and C_T doing so also. The pressure derivative of C_L increases with x except for a slight minimum at $x=0.21$, while $\partial C_T/\partial P$ goes through a maximum between $x=0.11$ and $x=0.21$.

A modified Born criterion for structural stability under pressure, developed by Demarest *et al.*,²⁴ states that the ratio of the shear modulus to the bulk modulus, C_T/B , should reach a small value at the pressure where a structural phase transition involving macroscopic shear occurs. This critical value is between 0.15 and 0.20 for crystalline materials most similar to our samples in chem-

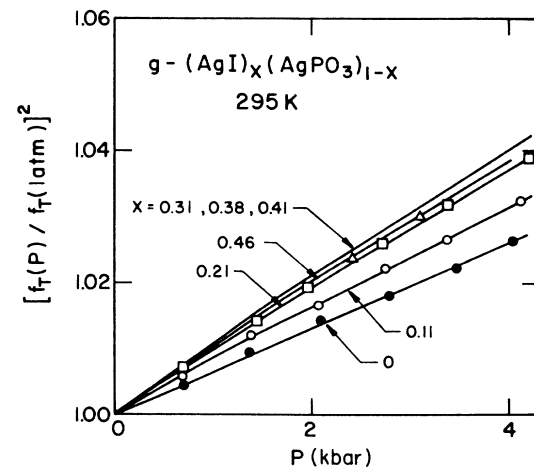


FIG. 6. The pressure dependence of the square of the transverse wave echo-overlap frequency, f_T^2 , in $(\text{AgI})_x(\text{AgPO}_3)_{1-x}$ glasses at room temperature for several values of x . All f_T^2 values were measured at 5 MHz.

ical composition. Figure 7 shows that, in all of our samples, the ratio C_T/B decreases markedly with increasing pressure, falling as low as 0.207 at 3.3 kbar in the $x=0.46$ sample. The reason for not presenting C_T/B values at pressures greater than 3.3 kbar for this sample is that the ultrasonic shear wave echoes disappeared near that pressure and did not reappear as pressure was increased up to almost 4 kbar. We do not think a structural transition caused the echo loss because: (1) as the pressure was decreased the echoes reappeared at about 3.3 kbar and the same overlap frequencies were observed with decreasing pressure as had been obtained with increasing pressure and (2) after the sample was removed its appearance was the same as before the pressure run.

We do think that structural stability vanishes at a higher pressure than we could achieve. In order to deduce the value of this pressure we shall use the Demarest *et al.* criterion. However, instead of simply employing the limiting C_T/B values mentioned above, we shall use our elastic moduli *versus* AgI content data to deduce a critical value for C_T/B . In order to do so we made a linear extrapolation of our C_T and C_L values up to the fractional AgI content ($x=0.65$) at which our $(\text{AgI})_x(\text{AgPO}_3)_{1-x}$ glasses could no longer be prepared by casting the melt into a mold. Since $C_T=0.99(1-0.88x)\times 10^{11}$ dyn/cm² and $C_L=5.0(1-0.67x)\times 10^{11}$ dyn/cm², then $B=3.67(1-0.60x)\times 10^{11}$ dyn/cm². This results in $C_T/B=0.19$ at $x=0.65$. Note that 0.19 is within the range of values expected from data on crystalline compounds.²⁴ Now we estimate the pressure, P_t at which structural stability is expected to vanish in our $x=0.46$ sample. Since C_T and C_L (and thus B) were observed to increase linearly with pressure we calculate P_t to be 7.6 kbar by means of the relation

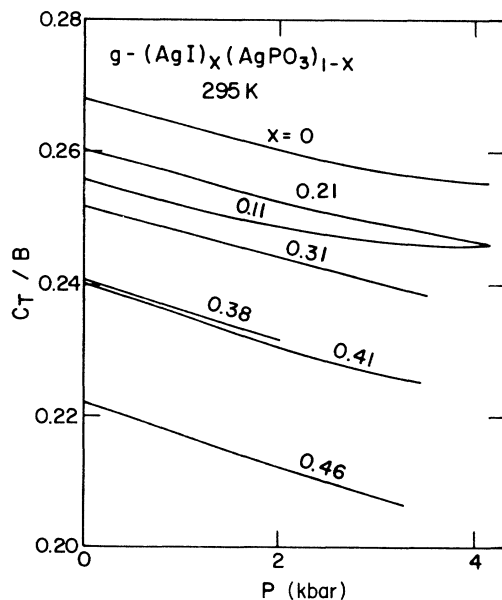


FIG. 7. The pressure dependence of the ratio C_T/B in $(\text{AgI})_x(\text{AgPO}_3)_{1-x}$ glasses at room temperature for several values of x . All values were measured at 5 MHz.

$$0.19 = (C_T/B)_{\text{crit}} = \frac{0.59(1 + 1.184 \times 10^{-2} P_t)}{2.662(1 + 3.575 \times 10^{-2} P_t)} \quad (14)$$

in which P_t is expressed in kbar.

In order to compare this transition pressure with the effect of AgI content on structural stability we calculated an effective internal pressure from the difference between the 5.679 g/cm³ density obtained by extrapolating our measured densities up to $x=0.65$, using the expression $\rho=4.45(1-0.425x)$ g/cm³, with the 5.419 g/cm³ value calculated from the molar masses and volumes of α -AgI and of AgPO_3 glass. We used the relation $P_{\text{effect}} = B \Delta\rho/\rho$, where B is the bulk modulus and ρ the density to obtain

$$P_{\text{effect}} = 2.24 \left[\frac{5.679 - 5.419}{5.419} \right] 10^{11} \text{ dyn/cm}^2 = 11 \text{ kbar} . \quad (15)$$

This value of P_{effect} is in reasonable agreement with the value of P_t obtained above since P_t is quite sensitive to the limiting value chosen for C_T/B . (For example, a value of 0.18 yields $P_t = 11$ kbar.)

For AgPO_3 we obtain, using its moduli and their pressure dependences, $P_t \approx 43$ kbar if $(C_T/B)_{\text{crit}} = 0.19$ and, of course, intermediate AgI content samples are expected to have P_t 's between this value and that of the $x=0.46$ sample.

From Fig. 7 we see that C_T/B decreases with increasing pressure for AgPO_3 glass, and that the greater the AgI content the stronger the decrease in C_T/B with increasing pressure. This behavior seems to indicate that a weakening (or some disruption) of the cross-linking between the chains of PO_4 tetrahedra is involved.

One sample (31 mol % AgI) was also studied as a function of pressure at 196 K. We found that $\partial C_L/\partial P$ was 9.56 at 196 K, whereas it was 9.37 at room temperature. However, $\partial C_T/\partial P$ has a value of 0.74 at 196 K and 0.85 at room temperature. Hence, the pressure derivative of the ratio C_T/B at low pressures actually decreases slightly from -0.37×10^{-11} cm²/dyn at 296 K to -0.47×10^{-11} cm²/dyn at 196 K. This would imply that the structure is slightly less stable at lower temperatures.

Crystalline AgI in the wurtzite (β) phase shows an unusual hysteretic behavior in the pressure dependence of its elastic constants.¹² This is thought to be associated with some restacking of lattice layers in the process of conversion to the zinc-blende phase. None of our samples showed any sign of hysteresis during pressure cycling. This is consistent with Malugani and Mercier's proposal²⁵ that the AgI regions form in the α phase, rather than the usual room temperature β phase.

F. Explicit temperature dependence of elastic moduli

The pressure derivatives of the elastic constants C_j can be used to calculate the implicit dilatational contribution to the temperature dependence of the elastic constants, i.e., $-3aB(\partial \ln C_j/\partial P)_T$, where a is the linear-expansion coefficient and B the bulk modulus. Then using the ex-

perimental temperature dependences of the elastic constants $(\partial \ln C_j / \partial T)_P$ and the relation

$$\left[\frac{\partial \ln C_j}{\partial T} \right]_P = -3aB \left[\frac{\partial \ln C_j}{\partial P} \right]_T + \left[\frac{\partial \ln C_j}{\partial T} \right]_V \quad (16)$$

we can deduce the explicit temperature dependence of each modulus $(\partial \ln C_j / \partial T)_V$ at room temperature. These values are summarized in Table II.

We found that the dilatational contribution to the temperature dependence of C_L is large, but nearly independent of AgI concentration. The explicit thermal contribution increases in importance with increasing AgI content, until it is comparable to the dilatational term.

The explicit temperature derivative of C_T is negative and much larger in magnitude than the dilatational contribution, which decreases (becomes more negative) slowly with AgI content relative to the explicit thermal contribution.

G. Elastic Grüneisen parameters

The elastic Grüneisen parameters for the long-wavelength longitudinal- and transverse-acoustic modes, γ_L and γ_T , respectively, may be determined^{26,27} from the values of the moduli and their pressure dependencies using

$$\gamma_{L,T} = \frac{B}{2C_{L,T}} \left[\frac{\partial C_{L,T}}{\partial P} \right]_T^{-\frac{1}{6}}. \quad (17)$$

These values are summarized in Table III. The values of γ_L increase monotonically with increasing x except for the $x=0.31$ sample. The shear mode Grüneisen parameters, γ_T , rise from 1.18 at $x=0$ to 1.54 at $x=0.11$ before falling back to 1.41 at $x=0.46$. The strongly positive values of γ_L are a consequence of hydrostatic pressure causing the longitudinal-acoustic modes to stiffen; this is normal behavior in the sense that it means that the energies of these modes are raised when the glass is compressed isotropically. The behavior of γ_T may be the result of AgI both weakening interchain interactions, as

indicated by the elastic constant values, and performing a space-filling role, as indicated by the density increasing faster than a simple volume-replacement model would allow.

Our Grüneisen parameter values are in marked contrast to those observed in the related system of $(\text{AgI})_x[(\text{Ag}_2\text{O})_{0.33}(\text{B}_2\text{O}_3)_{0.67}]_{1-x}$ glasses,²⁸ in which γ_L rises from 0.95 at $x=0.1$ to 1.98 at $x=0.6$, and γ_T decreases from -0.19 at $x=0.1$ to -0.4 at $x=0.6$. The negative Grüneisen parameters of this system have been attributed to the open structure which allows bending vibrations involving the bridging oxygen ions.

For an isotropic substance at temperatures well below the Debye temperature where only long-wavelength non-dispersive acoustic modes are excited, the mean thermal Grüneisen parameter γ_{th} would have a limiting value γ_S^0 given by²⁶

$$\gamma_S^0 = \frac{(V_T/V_L)^2 \gamma_L + 2\gamma_T}{(V_T/V_L)^3 + 2}. \quad (18)$$

The values of γ_S^0 listed in Table III were calculated using room-temperature velocities. They increase by less than 2% when recalculated with projected low-temperature velocities. We do not expect γ_S^0 to approach the Grüneisen thermal parameter γ_{th} at low temperatures because glassy tunneling modes will probably make a relatively larger contribution to γ_{th} at low T than they do at higher temperatures.

At high temperatures the long-wavelength, nondispersive acoustic modes would yield an average Grüneisen parameter γ_S^∞ equal to $(\gamma_L + 2\gamma_T)/3$. As can be seen in Table III, our values of γ_S^∞ are much larger than the Grüneisen parameters deduced from our elastic constant versus temperature data or from the thermal expansivity. This indicates that modes with negative Grüneisen parameters must still be of some importance at room temperature. Recall that our thermal-expansivity data indicated that negative Grüneisen parameter modes must predominate below 153 or 140 K in the $x=0$ and $x=0.31$ samples, respectively.

TABLE II. Experimental temperature derivative of the logarithm of each elastic modulus, the dilatational contribution to the temperature dependence, and the explicit thermal contribution for $(\text{AgI})_3(\text{AgPO}_3)_{1-x}$ glasses at 295 K. (Units are 10^{-4} K^{-1} .)

x	Modulus	$\left[\frac{\partial \ln C_j}{\partial T} \right]_P$	$-3aB \left[\frac{\partial \ln C_j}{\partial P} \right]_T$	$\left[\frac{\partial \ln C_j}{\partial T} \right]_V$
0.00	C_L	$-6.01 \pm 0.5\%$	$-4.30 \pm 8\%$	-1.71
	C_T	-8.01	-1.86	-6.15
0.11	C_L	-7.29	-4.92	-2.37
	C_T	-10.38	-2.36	-8.02
0.31	C_L	-10.44	-4.84	-5.60
	C_T	-14.39	-2.33	-12.06
0.39	C_L	-8.53	-5.08	-3.45
	C_T	-14.9	-2.24	-12.66

TABLE III. Room-temperature longitudinal and shear mode elastic Grüneisen parameters γ_L and γ_T , low- and high-temperature acoustic mode Grüneisen parameters derived from the room temperature γ_L and γ_T , and elastic Debye temperatures from room-temperature data for $(\text{AgI})_x(\text{AgPO}_3)_{1-x}$ glasses.

x	γ_L	γ_T	γ_S^0	γ_S^∞	Θ_{el}
0.00	2.95	1.18	1.26	1.77	208
0.11	3.40	1.54	1.62	2.16	191
0.21	3.43	1.53	1.61	2.16	176
0.31	3.34	1.52	1.60	2.13	162
0.39	3.52	1.46	1.53	2.14	149
0.41	3.63	1.48	1.56	2.19	143
0.46	3.88	1.41	1.49	2.23	135

IV. CONCLUSIONS

From measurements of ultrasonic transit times and thermal expansivity we have found the following for $(\text{AgI})_x(\text{AgPO}_3)_{1-x}$ glasses.

(1) Structural stability is reduced by the presence of AgI or the application of hydrostatic pressure.

(2) The shear-to-bulk modulus ratio is close to that expected for material containing a (quasi-) one-dimensional backbone and an interstitial fluid.

(3) The ultrasonic velocity is reduced by Ag-ion relaxation.

(4) The anharmonicity parameters (Grüneisen parameters) of long-wavelength acoustic modes (deduced from pressure dependences of the elastic constants) are larger than the room temperature values of the anharmonicity parameters deduced from the temperature dependences of the elastic constants or the Grüneisen parameter obtained from the thermal expansivity.

(5) The thermal expansion coefficient becomes negative

below a surprisingly high temperature.

Finding (1) implies that structural stability decreases and that a phase transition involving macroscopic shear may occur at a higher pressure, P_t , than we were able to achieve. We deduce that P_t decreases from about 43 kbar for our AgPO_3 glass sample to about 8 kbar for our $x=0.46$ sample. Finding (2), we think, is a consequence of the presence of chains of corner-connected PO_4 tetrahedra with Ag or AgI between the chains. Findings (4) and (5) imply that there are excitations with a negative anharmonicity parameter as well as vibrational modes with positive Grüneisen parameters.

ACKNOWLEDGMENTS

The initial part of this work was supported in part by the National Science Foundation via Grant No. DMR-79-08538-A3 and the Materials Research Laboratory (MRL) Program Grant No. DMR-83-16988.

¹C. A. Angell, *Solid State Ions*, **9-10**, 3 (1983).

²C. Liu and C. A. Angell, *J. Non-Cryst. Solids* **83**, 162 (1986).

³S. Radhakrishna (private communication).

⁴M. B. M. Mangion and G. P. Johari, *Phys. Chem. Glass* **29**, 225 (1988).

⁵L. Börjesson, S. W. Martin, L. M. Torell, and C. A. Angell, *Solid State Ionics* **18&19**, 431 (1986).

⁶E. Bogue, Ph.D. thesis, Purdue University, 1989.

⁷R. Truell, C. Elbaum, and B. Chick, *Ultrasonic Methods in Solid State Physics* (Academic, New York, 1969), pp. 161ff and Appendix H.

⁸C. L. Liu (private communication).

⁹H. J. McSkimin and P. Andreatch, *J. Acoust. Soc. Am.* **34**, 609 (1962).

¹⁰E. P. Papadakis, *J. Acoust. Soc. Am.* **42**, 1045 (1967).

¹¹R. K. Cook, *J. Acoust. Soc. Am.* **29**, 445 (1957).

¹²T. A. Fjeldly and R. C. Hanson, *Phys. Rev. B* **10**, 3569 (1974).

¹³R. F. Bartholomew, *J. Non-Cryst. Solids* **7**, 221 (1972).

¹⁴T. Minami, T. Katsuda, and M. Tanaka, *J. Phys. Chem.* **83**, 1306 (1979).

¹⁵W. B. Daniels, in *Report of the International Conference on the Physics of Semiconductors, Exeter, 1962*, edited by A. C. Strickland (Institute of Physics—The Physical Society, London, 1962), p. 482.

¹⁶V. K. H. Jost, *Acta Crystallogr.* **14**, 779 (1961).

¹⁷G. Carini, M. Cutroni, A. Fontana, G. Mariotto, and F. Rocca, *Phys. Rev. B* **29**, 3567 (1984).

¹⁸D. N. Nichols, D. S. Rimai, and R. J. Sladek, *J. Non-Cryst. Solids* **34**, 297 (1979).

¹⁹O. K. Chan, F. C. Chen, C. L. Choy, and I. M. Ward, *J. Phys. D* **11**, 617 (1978).

²⁰D. J. Bergman and Y. Kantor, *Phys. Rev. Lett.* **53**, 511 (1984).

²¹G. Leibfried and W. Ludwig, in *Solid State Physics*, edited by F. Seitz and D. Turnbull (Academic, New York, 1956), Vol. 2, p. 276.

²²J. A. Garber and A. V. Granato, *Phys. Rev. B* **11**, 3990 (1975).

²³T. N. Claytor and R. J. Sladek, *Phys. Rev. B* **18**, 5842 (1978).

²⁴H. H. Demarest, Jr., R. Ota, and O. L. Anderson, in *High-Pressure Research Applications in Geophysics*, edited by M. H. Manghani (Academic, New York, 1977), p. 281.

²⁵J. P. Malugani and R. Mercier, *Solid State Ionics* **13**, 293 (1984).

²⁶C. S. Smith, D. E. Schuele, and W. B. Daniels, in *Physics of Solids at High Pressures*, edited by C. Tomizuka and R. Emrick (Academic, New York, 1965), p. 496.

²⁷K. Brugger and T. C. Fritz, *Phys. Rev.* **157**, 524 (1967).

²⁸G. A. Saunders, H. A. A. Sidek, J. D. Comins, G. Carini, and M. Federico, *Philos. Mag.* **B 56**, 1 (1987).